Zheng *et al. Chem. Biol. Technol. Agric.* (2024) 11:13
https://doi.org/10.1186/s40538-024-00538-4

Chemical and Biological Technologies in Agriculture

RESEARCH

Open Access

Analysis of the adsorption mechanism of phosphoric acid-modified bamboo charcoal for chlorogenic acid based on density functional theory

Wenxi Zheng[1], Sheng Zhang[1*] and Jing Deng[1]

Abstract

Background Bamboo charcoal has garnered wide recognition as an adsorbent owing to its stability and availability. Phosphoric acid modification contributes to forming specific functional groups on the surface of bamboo charcoal, culminating in the augmentation of its adsorption capabilities.

Results The modification process in this study involved impregnating the bamboo charcoal in a 45% mass fraction of phosphoric acid solution with a 1:10 ratio (bamboo charcoal powder to phosphoric acid), followed by activation at a temperature of 500 °C for a duration of 1.5 h. The modification resulted in the formation of hydroxyl, carboxyl, and phosphate groups on the surface of the bamboo charcoal. Furthermore, the specific surface area of the modified bamboo charcoal surged from 4.91 m^2/g to 115.18 m^2/g, the average aperture decreased from 7.15 nm to 1.99 nm, and the pore volume escalated by 6.5 times. On this basis, a comparison in the adsorption capability for chlorogenic acid, a natural small-molecule active ingredient, was drawn before and after the modification of bamboo charcoal. The results indicate that the modified bamboo charcoal showcases an impressive 46.8-fold increase in its adsorption capacity when juxtaposed with the unmodified bamboo charcoal. Through the calculations based on density functional theory (DFT), the addition of functional groups on the surface of the modified bamboo charcoal module allows for the formation of hydrogen bonds with the chlorogenic acid module, with the highest binding energy reaching −57.59 kJ/mol.

Conclusion As evidenced by the adsorption kinetic studies, the curve of modified bamboo charcoal for chlorogenic acid abides by a first-order kinetic equation. Additionally, adsorption thermodynamic studies reveal that the curve of modified bamboo charcoal for chlorogenic acid conforms to the Boltzmann equation. These results shed light on the mechanism of selectively adsorbing specific constituents using phosphoric acid-modified bamboo charcoal, thereby providing a solid theoretical foundation for the application of bamboo charcoal.

Keywords Phosphoric acid modification, Bamboo charcoal, Chlorogenic acid, Density functional theory, Adsorption

*Correspondence:
Sheng Zhang
gingshen123@126.com
Full list of author information is available at the end of the article

Graphical Abstract

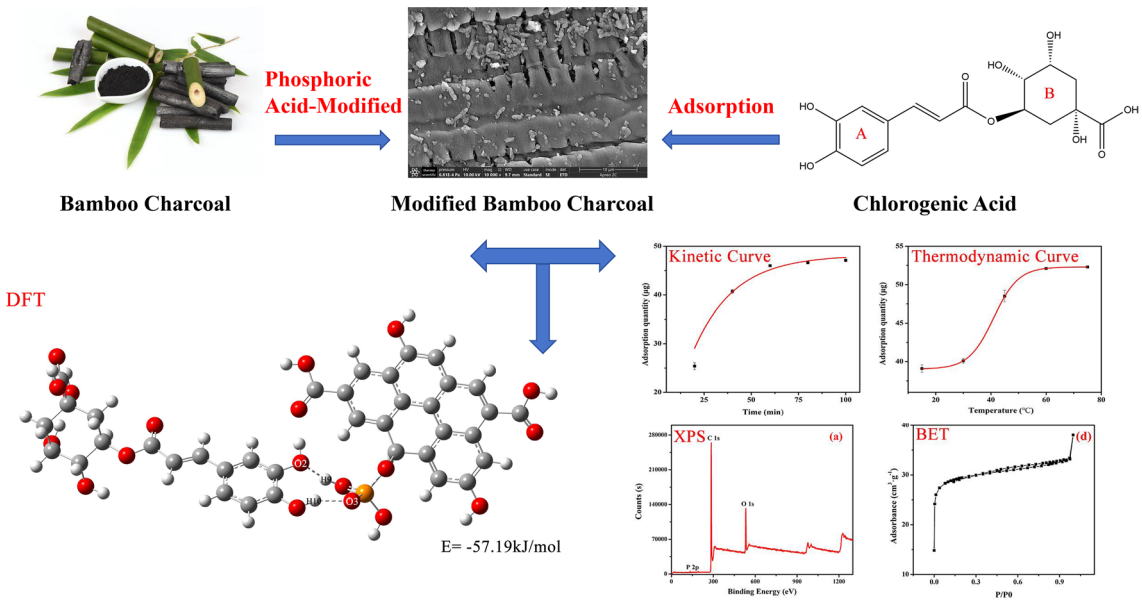

Introduction

Chlorogenic acid, a compound of phenylpropanoic acid with the formula $C_{16}H_{18}O_9$, functions as a natural active ingredient prevalently observed in industrial crops [1, 2] such as *Eucommia ulmoides* and *Acer truncatum*. Chlorogenic acid has various positive effects, including anti-aging [3], acne removal [4], skin whitening [5], anti-obesity [6], anti-diabetes [7], and anti-cancer [8]. However, high water solubility inherent in chlorogenic acid potentially leads to rapid diffusion and short-term effectiveness upon application. To address this issue, adsorbing chlorogenic acid onto a sustained-release material can extend its duration of action [9].

Bamboo charcoal is an absorbent used for the natural organic matters such as caffeic acid [10], quercetin [11], and *Eucommia ulmoides* leaf extract [12]. Although bamboo charcoal has a certain adsorption capacity, the application of untreated bamboo charcoal is impeded due to its lower surface area and poor functional groups [13]. To expand the application scope, bamboo charcoal needs to be activated and modified to become activated carbon. The modification process for activated carbon can be categorized into physical [14, 15] and chemical methods [16–18]. Albeit with simplicity, the physical modification falls short of precision in the selectivity of the adsorption target. Chemical modification, by contrast, can modify the surface functional groups according to the characteristics of the adsorbed components, thereby achieving precise adsorption. One commonly used method of chemical modification is the use of phosphoric acid [19]. Phosphoric acid demonstrates the capacity to augment the specific surface area and pore volume of activated carbon while introducing more functional groups on the surface.

Higai et al. [20] performed surface modification on coconut shells using phosphoric acid, highlighting the advantages of oxygen-containing functional groups on the surface for adsorption. Chen et al. [19] discovered that hydrothermal bamboo-derived biochar modified with phosphate groups not only effectively increases the specific surface area but also activates oxygen-containing functional groups on the surface. Ismail et al. [21] reported a substantial increase in the specific surface area of bamboo charcoal modified with phosphoric acid. However, there was no analysis of functional groups regarding bamboo charcoal modified with phosphoric acid.

Density Functional Theory (DFT) stands as a powerful tool in the field of condensed matter physics for determining electronic structures and their properties. Recent years have witnessed significant advancements in DFT, encompassing various aspects of material design, synthesis, analog computation, and evaluation, establishing itself as a crucial foundation and core technology in computational materials science. Zhang et al. explored the molecular interaction between the organic pollutant

and the aromatized biochar through adsorption experiments and DFT calculations [22]. Wang et al. elucidated the mechanism behind removing organic solvents from wastewater using a composite material consisting of bamboo charcoal and polyurethane foam through DFT [23]. Additionally, Feng et al. employed DFT to reveal both the performance and mechanism for effectively treating ammonia nitrogen pollution in rare earth ore by employing potassium permanganate and sodium silicate co-modified bamboo charcoal [24].

Presently, there is a dearth of DFT-based studies on the mechanism behind the adsorption of natural small-molecule active ingredients by activated carbon. To fill this gap, this study revolves around chlorogenic acid as a representative of natural small-molecule active ingredients. The adsorbent used is phosphoric acid-modified bamboo charcoal, which allows for a comparison of the adsorption capacity for chlorogenic acid before and after modification. The material characteristics analysis of the modified bamboo charcoal proceeds with various characterization methods such as Infrared Spectroscopy (IR), Brunauer–Emmett–Teller (BET) analysis, X-ray Diffraction (XRD), X-ray Photoelectron Spectroscopy (XPS), and Scanning Electron Microscopy (SEM). DFT is used to reveal the mechanism of phosphoric acid-modified bamboo charcoal on the adsorption of chlorogenic acid.

Materials and methods

Materials

This study utilized bamboo charcoal sourced from Hunan Xinsheng Bamboo Industry Co., Ltd., Hunan, China, and chlorogenic acid from Tianjin Yifang Technology Co., Ltd., Tianjin, China. Both bamboo charcoal and chlorogenic acid were of analytical grade. Moreover, this study also used phosphoric acid (Tianjin Hengxing Chemical Reagent Manufacturing Co., Ltd., Tianjin, China) and sodium hydroxide (Shanghai Wokai Biotechnology Co., Ltd, Shanghai, China), both of which were also of analytical grade.

Preparation of phosphoric acid-modified bamboo charcoal

The bamboo charcoal was crushed into smaller pieces and then sifted through a 20-mesh sieve. A specific amount of bamboo charcoal powder was accurately weighed and transferred into a 50-mL conical flask. Subsequently, the bamboo charcoal powder was thoroughly mixed with a 30%–60% mass fraction solution of H_3PO_4. The ratio of bamboo charcoal powder to phosphoric acid for impregnation ranged between 1:1 and 1:10, based on mass to volume, with an impregnation time of 24 h. The mixture of bamboo charcoal and phosphoric acid underwent filtration and subsequent modification in a tubular atmosphere furnace, maintaining temperatures between 500 and 700 ℃ for a duration spanning 1 to 2 h, accompanied by a continuous nitrogen gas flow. The YQG1100-80 tubular atmosphere furnace from Shanghai Yongqing Experimental Instrument Co., Ltd., Shanghai, China, was utilized for this purpose. The modified bamboo charcoal was neutralized using a 5% sodium hydroxide solution, rinsed with distilled water until it reached a neutral pH, and then dried at 105 °C for later use.

Table 1 Orthogonal experimental factors and levels ($L4^3$)

	A Mass fraction of phosphoric acid (%)	B Impregnation ratio	C Temperature (℃)	D Time (h)
1	30	1:1	500	1.0
2	45	1:5	600	1.5
3	60	1:10	700	2.0

Table 2 Absorbance values of chlorogenic acid at each concentration

Concentration *x* (μg/mL)	0.23	0.95	1.19	1.59	2.38
Absorbance *y*	0.136	0.662	0.812	1.091	1.602

To further investigate the process of preparing phosphoric acid-modified bamboo charcoal, this study selected four key factors that may influence the modification process, including the mass fraction of phosphoric acid (m), the impregnation ratio (℃), the activation temperature, and the activation time (h). Moreover, a systematic approach was employed, involving the design of a four-factor, three-level orthogonal test table (Table 1), guiding the subsequent experimentation.

Adsorption capability of bamboo charcoal for chlorogenic acid

Through experiments assessing the adsorption capacity of bamboo charcoal powder under diverse modification conditions while retaining a fixed concentration of chlorogenic acid solution, this study aimed to pinpoint the optimal modification conditions for bamboo charcoal. This study utilized a UV–Vis spectrophotometer (UV-1100/UV-1200, Macylab Instrument Inc., Shanghai, China) to measure the absorbance of chlorogenic acid solution. The changes in absorbance were used to calculate the adsorption capacity of bamboo charcoal. This process commenced by preparing various concentrations of aqueous solutions containing chlorogenic acid, followed by measuring their absorption values at a wavelength of 327 nm, as recorded in

Table 2. Analyzing the correlation between chlorogenic acid concentration and the respective absorption values allowed the establishment of a standard curve equation: $y = 0.6903x - 0.0020$ ($R^2 = 0.9991$).

On this basis, this study proceeded to assess the adsorption capacity of bamboo charcoal for chlorogenic acid via experiments. An appropriate amount of chlorogenic acid was accurately weighed and dissolved in deionized water to prepare a 2 μg/mL solution in a 100-mL beaker. Subsequently, 0.1 g of unmodified bamboo charcoal powder was added to the solution and stirred at 25 ℃ or 40 min using a magnetic stirrer (DF-101S, Yuhua Instrument Co., Ltd., Henan, China). Following this, 2 mL of the solution underwent extraction using a syringe and passed through a microporous membrane for filtration. The absorbance of the filtered solution was measured at a wavelength of 327 nm. After measurement, the solution was reinstated to its original container. The absorbance value was then leveraged in the equation of the standard curve to calculate the concentration of chlorogenic acid.

After determining the concentration of the chlorogenic acid solution before and after adding bamboo charcoal while keeping the volume constant, this study calculated the adsorption capacity of bamboo charcoal for chlorogenic acid as 1 μg using Formula 1. The modified bamboo charcoal was also measured using the same method.

$$M = (C_1 - C_2) \times 100. \quad (1)$$

This formula denotes M as the adsorption capacity of bamboo charcoal for chlorogenic acid (μg), C_1 as the concentration of the chlorogenic acid solution before adsorption (μg/mL), C_2 as the concentration of the chlorogenic acid solution after adsorption (μg/mL), and 100 as the volume of the chlorogenic acid solution used in this study (mL).

IR

IR analysis was performed by preparing the sample into potassium bromide pellets and scanning it using a Nicolet iS10 Fourier transform infrared spectrometer from Thermo Fisher Scientific, located in Massachusetts, U.S.A. The scan was conducted within the wavelength range of 400–4000 cm^{-1}.

BET

For BET analysis, the N_2 adsorption–desorption isotherms of the sample were measured using an ASAP 2460 full-automatic specific surface area and porosity analyzer from Micromeritics, Georgia, U.S.A. Nitrogen gas was used to test the pore size. The sample was prepared at a temperature of 700 °C and degassed at 300 °C.

XRD

XRD was used to determine the crystal structure and phase composition of the sample. The analysis was conducted using an X-ray diffractometer (Ultima IV, Rigaku Corporation, Tokyo, Japan) equipped with a copper target material. Wide-angle X-ray diffraction was performed within a scanning angle range of 5–85°, employing a scanning rate of 5°/min.

XPS

The chemical valence state, elemental composition, and relative abundance of the sample were analyzed by harnessing the ESCALAB Xi+XPS from Thermo Fisher Scientific in Massachusetts, U.S.A. The binding energies of each chemical constituent were calibrated using the binding energy of C 1s = 284.8 eV as the energy reference. The experimental conditions involved a vacuum pressure of $8 \times l0^{-10}$ Pa inside the analysis chamber. The source of excitation was Al Ka (1486.6 eV) radiation. The operating voltage and the filament current were set at 12.5 kV and 16 mA, respectively. The signal accumulation comprised ten cycles. For the complete spectrum, the pass energy used was 100 eV, while for the narrow spectrum, it was 30 eV. The step size was 0.05 eV, and the dwell time was between 40 and 50 ms.

SEM

An Apreo 2 SEM produced by Thermo Fisher Scientific in Massachusetts, U.S.A., was utilized to examine the surface microtopography of the modified bamboo charcoal. The material was uniformly affixed to a conductive adhesive and subjected to a vacuum for approximately 15 min. Utilizing a resolution of 1 nm and a voltage of 3 kV, the surface microtopography of the sample was observed at magnifications of $10^3\times$, $10^4\times$, and $10^5\times$.

DFT calculations

The molecular configuration of chlorogenic acid was sourced from PubChem [25], while the molecular structure of activated carbon was typically simulated using graphene [26]. The molecular structure of modified bamboo charcoal was constructed based on characterization results.

In line with DFT, this study optimized the structure of the functional groups on the chlorogenic acid molecule and the modified bamboo charcoal molecule using the B3LYP method with a 6–31+G (d, p) basis in Gaussian 16 [27]. The calculation of the binding energy, E, was conducted using Formula 2. Additionally, ΔE_{BSSE}, the basis set superposition error, was calculated using Boys and Bernardi's function counterpoise procedure [28].

$$E = E_{BE} - (E_c + E_b) + \Delta E_{BSSE} \quad (2)$$

The formula mentions E_{BE} as the total energy of the formed complex upon molecular binding, E_c as the relative energy of the chlorogenic acid molecule, and E_b as the relative energy of the modified bamboo charcoal module.

Eventually, this study employed Multiwfn [29], a multifunctional program for wavefunction analysis, and visual molecular dynamics (VMD) [30], a molecular visualization program, to visualize and analyze the binding of the modified bamboo charcoal module and the chlorogenic acid molecule.

Results

Optimal conditions for phosphoric acid-modified bamboo charcoal

The results from the orthogonal experimental design outlined in Part 2.2 and the analysis of variance (ANOVA) are shown in Tables 3 and 4, respectively.

The experiments proceeded with different combinations of conditions, ultimately identifying the optimal setting detailed in Table 3, denoted as $A_2B_3C_1D_2$. This suggests employing a 45% mass fraction of phosphoric acid, an impregnation ratio of 1:10, an activation temperature of 500 °C, and an activation duration of 1.5 h. Under these conditions, the adsorption capacity for chlorogenic acid peaked at 46.8 μg, marking a remarkable 46.8-fold increase compared to unmodified bamboo charcoal. The ANOVA in Table 4 confirms that the mass fraction of phosphoric acid has a significant impact on the adsorption capacity of chlorogenic acid.

Adsorption kinetics of modified bamboo charcoal for chlorogenic acid

A concentration of 2 μg/mL was dissolved in deionized water using a beaker to prepare a 100 mL solution. Afterward, 0.1 g of modified bamboo charcoal powder was added to the solution, and the adsorption was carried out at room temperature using a heat-collection constant-temperature magnetic stirrer. At intervals of 20 min, 40 min, 60 min, 80 min, and 100 min, 2 mL of solution was extracted using a syringe, filtered through a microporous membrane, and measured for absorbance at

Table 3 Intuitive Analysis of Orthogonal Experiments

No	Mass fraction of phosphoric acid (%)	Impregnation ratio	Temperature (℃)	Time (h)	Adsorption capacity for chlorogenic acid (μg)
1	30	1:1	500	1.0	7.6
2	30	1:5	600	1.5	4.8
3	30	1:10	700	2.0	37
4	45	1:1	600	2.0	40.8
5	45	1:5	700	1.0	38.4
6	45	1:10	500	1.5	46.8
7	60	1:1	700	1.5	34.6
8	60	1:5	500	2.0	41.2
9	60	1:10	600	1.0	31.8
k1	16.467	27.667	31.867	25.933	
k2	42.000	28.133	25.800	28.733	
k3	35.867	38.533	36.667	39.667	
R	25.533	10.866	10.867	13.734	

Table 4 ANOVA for orthogonal experiments

Factor	Sum of squares for error	Degree of freedom	*F*-ratio	*F*-statistic	Significance
Mass Fraction of Phosphoric Acid (%)	1,065.929	2	5.991	19.000	*
Impregnation Ratio	226.462	2	1.273	19.000	
Temperature (℃)	177.929	2	1.000	19.000	
Time (h)	315.982	2	1.776	19.000	
Error	177.93	2			

Table 5 Adsorbed amount (μg) of chlorogenic acid by modified bamboo charcoal at various time points ($n=3$)

No	20 min	40 min	60 min	80 min	100 min
1	24.8	40.4	45.8	46.6	46.8
2	25.2	40.6	46.2	46.8	47.4
3	26.2	41.2	46.0	46.4	47.2
$\overline{X}\pm$SD	25.4 ± 0.72	40.7 ± 0.41	46.0 ± 0.20	46.6 ± 0.20	47.1 ± 0.31

Table 6 Adsorbed amount (μg) of chlorogenic acid by modified bamboo charcoal at different temperature points ($n=3$)

No	15 ℃	30 ℃	45 ℃	60 ℃	75 ℃
1	38.6	39.8	47.6	52.0	52.4
2	39.0	40.4	49.0	52.2	52.2
3	39.6	40.2	48.8	52.2	52.2
$\overline{X}\pm$SD	39.1 ± 0.50	40.1 ± 0.31	48.5 ± 0.76	52.1 ± 0.12	52.3 ± 0.12

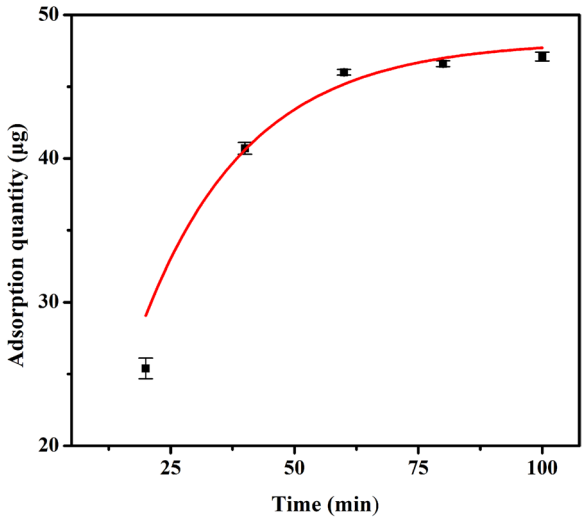

Fig. 1 Adsorption kinetic curve of chlorogenic acid

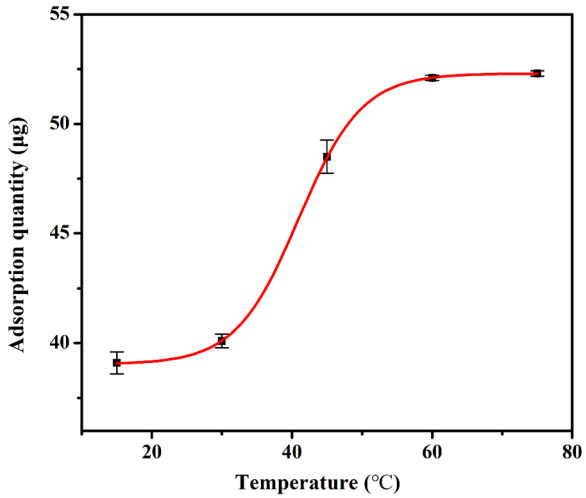

Fig. 2 Adsorption thermodynamic curve of chlorogenic acid

327 nm. After measurement, the solution was returned to its original container. By applying the equation from the standard curve for absorbance values, the concentration of chlorogenic acid in the adsorbed solution was calculated. The amount of chlorogenic acid adsorbed was calculated using Formula 1. The tabulated experimental findings are outlined in Table 5.

From Fig. 1, it is evident that modified bamboo charcoal exhibits a notable adsorption effect on chlorogenic acid. The adsorption capacity reached 46.0 μg at 60 min, after which the adsorption rate slowed down at 80 min. Subsequently, the adsorption curve gradually approached a plateau, signifying equilibrium in the adsorption process. Through the Curve Fitting in Origin, the curve follows a first-order kinetic equation, $y=48.180\ (1-e^{-0.046x})$, with a correlation coefficient of $R^2=0.9309$.

Adsorption thermodynamics of modified bamboo charcoal for chlorogenic acid

Five aliquots with a concentration of 2 μg/mL were dissolved in deionized water using a beaker to prepare five solutions of 100 mL. Afterward, 0.1 g of modified bamboo charcoal powder was added to the solutions. The solutions were subjected to constant stirring at temperatures of 15 ℃, 30 ℃, 45 ℃, 60 ℃, and 75 ℃ for 60 min using a heat-collection constant-temperature magnetic stirrer. A 2-mL sample of solution was extracted using a syringe, filtered through a microporous membrane, and measured for absorbance at 327 nm. The concentration of chlorogenic acid in the adsorbed solution was calculated, and the adsorption amount was determined using Formula 1. The experimental results are shown in Table 6.

Upon analyzing Fig. 2, it is evident that modified bamboo charcoal exhibited slow adsorption of chlorogenic acid at temperatures ranging from 15 °C to 30 °C. However, a notable acceleration in the adsorption rate occurred at temperatures between 30 °C and 60 °C. Subsequently, the adsorption rate decreased again in the temperature range of 60 °C to 75 °C, ultimately stabilizing at a steady state. Through the Curve Fitting in Origin, the curve follows the Boltzmann equation, $Y=\frac{-13.263}{1+e^{\frac{x-40.957}{4.51}}}+52.30$, with a correlation coefficient of $R^2=0.9999$.

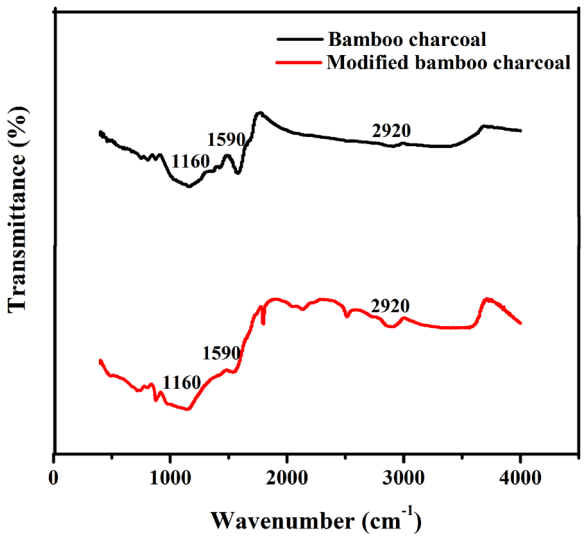

Fig. 3 IR spectra of modified bamboo charcoal

IR analysis

The IR spectra of bamboo charcoal and modified bamboo charcoal are illustrated in Fig. 3. Figure 3 demonstrates an absorption due to C–H stretching vibrations between 2800 and 3300 cm^{-1}. Above the wavenumber of 3000 cm^{-1}, absorption due to C–H stretching vibrations indicates the presence of unsaturated hydrocarbons. The intense spectral bands from wavenumbers 1590 cm^{-1} and 1160 cm^{-1} in unmodified bamboo charcoal are engendered by the stretching and bending vibrations of C–H bonds in the methyl ($–CH_3$) groups. However, for the modified bamboo charcoal, the stretching vibrations are significantly reduced, indicating substantial removal of hydrogen. Meanwhile, the presence of $–CH_2$ is indicated by the distinct peak observed near 2920 cm^{-1} in the bamboo charcoal.

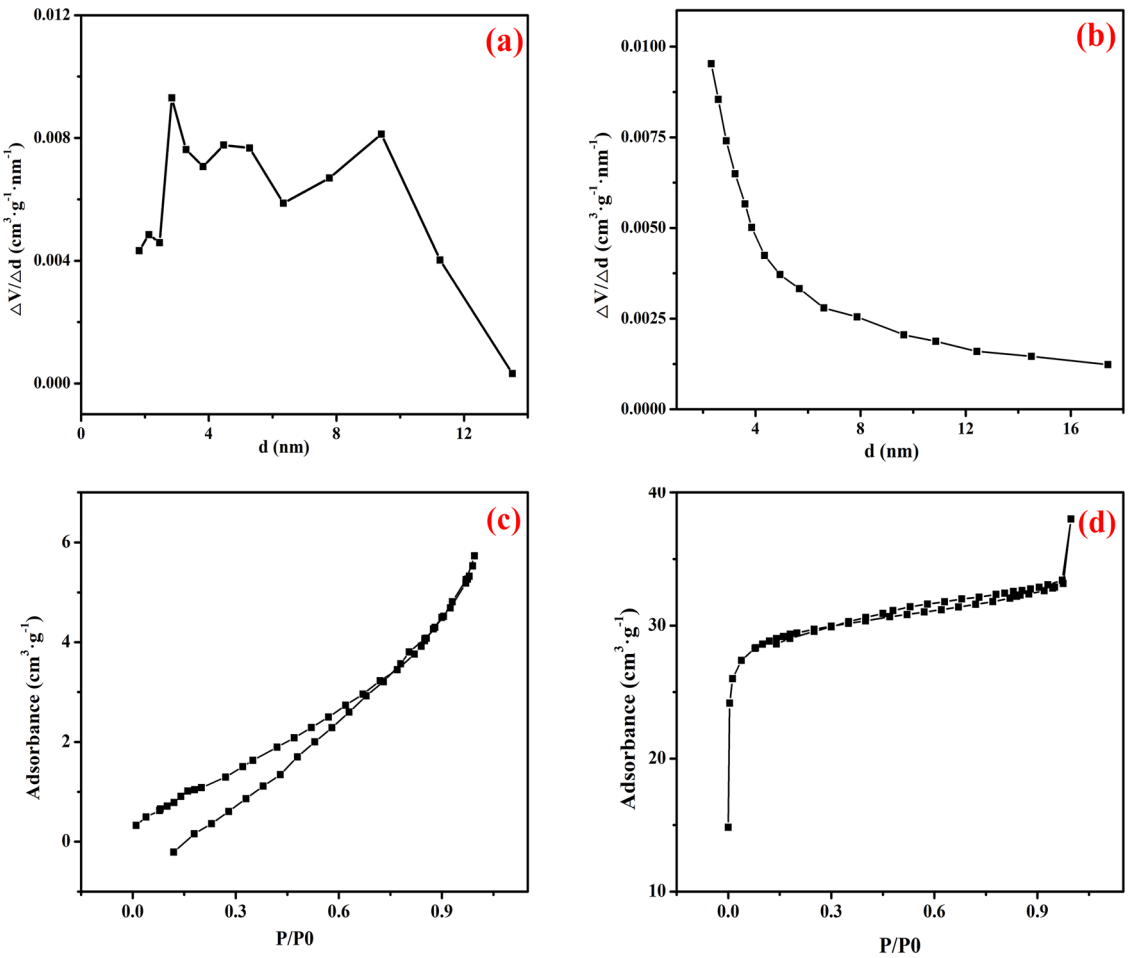

Fig. 4 Plot of aperture distribution of bamboo charcoal (**a**) and modified bamboo charcoal (**b**) and adsorption–desorption isothermal curves of bamboo charcoal (**c**) and modified bamboo charcoal (**d**)

BET analysis

The Barrett–Joyner–Halenda (BJH) analysis yields information about the aperture distribution curve and the adsorption–desorption isothermal curve for both unmodified and modified bamboo charcoal, as displayed in Fig. 4. Comprehensive details about the specific surface area and pore structure pre- and post-modification are documented in Table 7 for reference.

The specific surface area of unmodified and modified bamboo charcoal was 4.91 m^2/g and 115.18 m^2/g, respectively. This enhancement signifies a remarkable 23.5-fold augmentation compared to the unmodified variant. The total pore volume of unmodified and modified bamboo charcoal was 0.0088 cm^3/g and 0.0574 cm^3/g, respectively. This indicates that the modified bamboo charcoal has a pore volume 6.5 times greater than that of unmodified bamboo charcoal. Additionally, the average aperture of unmodified and modified bamboo charcoal was 7.15 nm and 1.99 nm, respectively. These results suggest that the modified bamboo charcoal has a larger total pore volume and a smaller average aperture, providing larger space and more opportunities for adsorption.

According to the physical adsorption characterization published by the International Union of Pure and Applied Chemistry (IUPAC), Figure (c) fits a Type IV isotherm with a hysteresis loop. This indicates that the unmodified bamboo charcoal has an irregular pore structure with no distinct saturation plateau. Figure (d), by contrast, represents the adsorption–desorption isothermal curves of modified bamboo charcoal, conforming to the Type I isotherm. Type I isotherms demonstrate an expedited rise in adsorption at lower relative pressures, reaching adsorption saturation at a certain relative pressure. Generally, Type I isotherms reflect the micropore filling of microporous adsorbents like molecular sieves and microporous activated carbon. In accordance with the IUPAC definition, micropores, mesopores, and macropores have apertures less than 2 nm, between 2 and 50 nm, and greater than 50 nm, respectively. Given the average aperture of 1.99 nm for the modified bamboo charcoal in this study, it predominantly comprises micropores and aligns with the Type I adsorption–desorption isotherms.

Table 7 Structure characteristics of modified bamboo charcoal

Sample	Specific surface area (m^2/g)	Pore volume (cm^3/g)	Adsorption isotherm	Average aperture (nm)
Modified bamboo charcoal	115.18	0.0574	Type I	1.99
Unmodified bamboo charcoal	4.91	0.0088	Type VI	7.15

XRD analysis

To confirm the crystalline or amorphous structure of bamboo charcoal before and after modification, X-ray diffraction (XRD) of the unmodified and modified bamboo charcoal was observed on X-ray diffractometer. The XRD pattern is presented in Fig. 5. Typically, a broad peak of the unmodified and modified bamboo charcoal position at $2\theta = 23.8$ was observed for all samples and corresponds to reflections of the (002) planes, respectively. The d was determined from the brag equation as expressed in Formula 3:

$$d = \frac{\lambda}{2sin\theta}, \tag{3}$$

where λ is the X-ray wavelength ($\lambda = 0.15406$ nm), and θ is the scattering angle for a particular peak position.

The crystallinity recorded was in the range of 8.6 with 91.4 amorphous. The reported values for the interlayer spacing, d_{002}, remain virtually unchanged with temperature and IR ratio. We obtained values that were in the range of 0.373, slightly higher than the graphite (0.335).

This result is similar to that of Pam et al. [31], indicating the existence of the (002) crystal plane of graphite. This observation implies that bamboo charcoal maintains a turbostratic graphite-like structure with excellent chemical and thermal stability.

XPS analysis

XPS analysis is a commonly used technique for identifying the elements in a material as well as their atomic ratios and chemical states. Figure 6 presents the complete

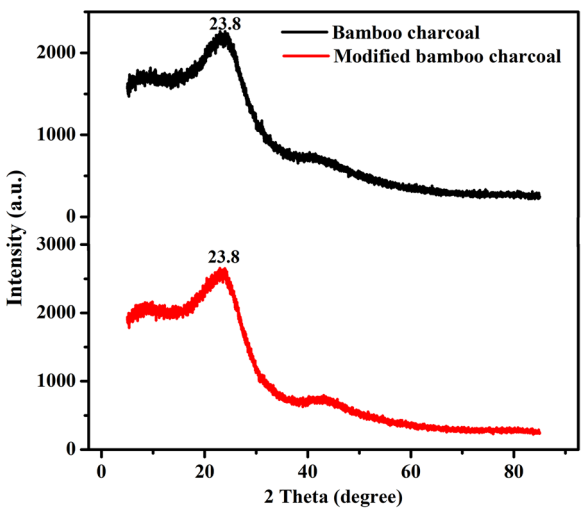

Fig. 5 XRD of modified bamboo charcoal

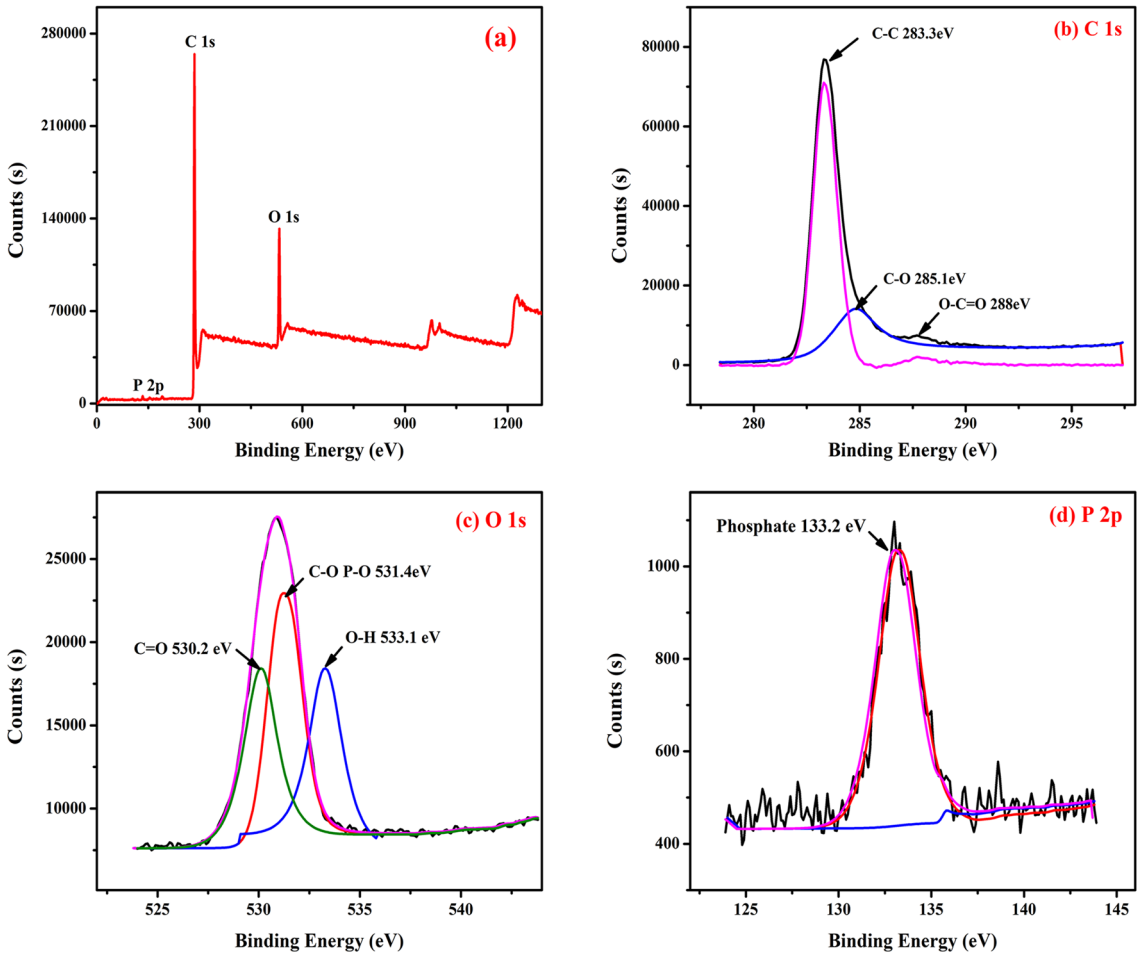

Fig. 6 Complete spectrum of bamboo charcoal (**a**) and high-resolution spectra of C 1s (**b**), O 1s (**c**), and P 2p (**d**) of modified bamboo charcoal

spectrum and high-resolution XPS spectra of modified bamboo charcoal. The C 1s spectrum (b) shows that the energy levels of C–C, C–O, and O=C–O are 283.3, 285.1, and 288.0 eV, respectively. The O 1s spectrum (c) shows energy levels of 530.2, 531.4, and 533.1 eV for C=O, C–O/P–O, and C–OH, respectively. The P 2p spectrum (d) shows an energy level of 133.2 eV for phosphate. By combining these results with those from the IR analysis, it can be concluded that the modified bamboo charcoal is chiefly composed of carboxyl, hydroxyl, and phosphate groups.

SEM analysis

The SEM analysis revealed the presence of pores in both unmodified and modified bamboo charcoal. Figure 7 shows these pores in the structure. The modification of bamboo charcoal with phosphoric acid resulted in a rougher surface texture, increased debris within the voids, and a proliferation of porous structures distributed along the walls of existing pores. The formation of these pores was attributable to the erosion process of phosphoric acid modification and the removal of phosphate compounds. The increased number of pores in the modified bamboo charcoal enhances its adsorption performance.

DFT calculations

Natural bond orbital (NBO) analysis

The NBO charges over atoms provide a useful approach for examining the nucleophilic or electrophilic characteristics of the reactive regions in molecules. Figure 8 illustrates the planar structures of the simulated chlorogenic acid molecule and the modified bamboo charcoal

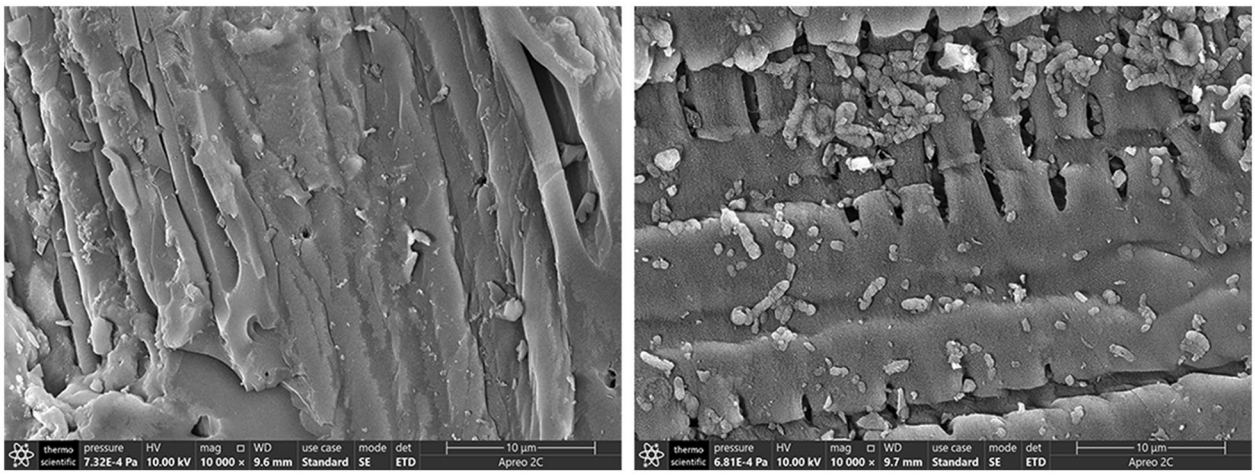

Fig. 7 SEM of bamboo charcoal (**a**) and modified bamboo charcoal (**b**)

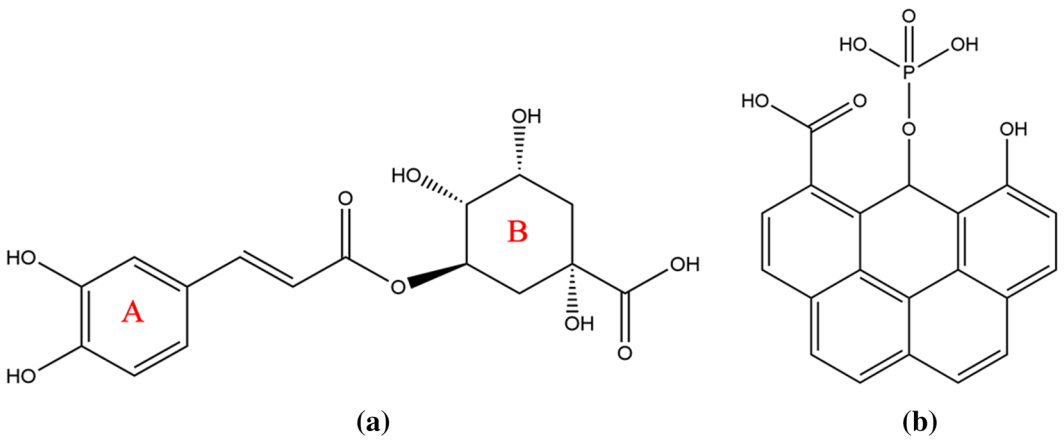

Fig. 8 Planar structures of the simulated chlorogenic acid molecule **(a)** and the Modified bamboo charcoal molecule (**b**)

molecule. Additionally, Fig. 9 showcases the NBO charge distribution on the surfaces of the simulated chlorogenic acid module and the modified bamboo charcoal molecule.

The molecular structure of chlorogenic acid is indicated in Fig. 8a. According to the data gathered from IR and XPS, the modified bamboo charcoal was simulated as graphene with hydroxyl, carboxyl, phosphate, and other functional groups, as depicted in Fig. 8b. The NBO charges over the surface functional groups of the simulated chlorogenic acid module and the modified bamboo charcoal module were calculated using the Gaussian 16 program, as shown in Fig. 9. Based on the data presented in Fig. 9a, it is evident that the oxygen atoms serve as electron donors in the chlorogenic acid molecule. The O1 and O2 atoms, located on the hydroxyl group of ring A, as well as the O7 atom on the hydroxyl group of ring B, are the three strongest donors. The NBO charges for these atoms are −0.526, −0.608, and −0.560, respectively. The hydrogen atoms, by contrast, act as electron acceptors in the chlorogenic acid molecule. The H10 and H11 atoms, found on the hydroxyl group of ring A, along with the H19, H21, H24, and H25 atoms on the hydroxyl group of ring B, function as strong acceptors, with NBO charges for these atoms of 0.387, 0.382, 0.358, 0.380, 0.390, and 0.386, respectively, which are markedly higher than the hydrogen atoms directly connected to the carbon atoms. The data from Fig. 9b indicate that on the modified bamboo charcoal, the oxygen atoms are all strong electron donors, and the NBO charges of H8, H9,

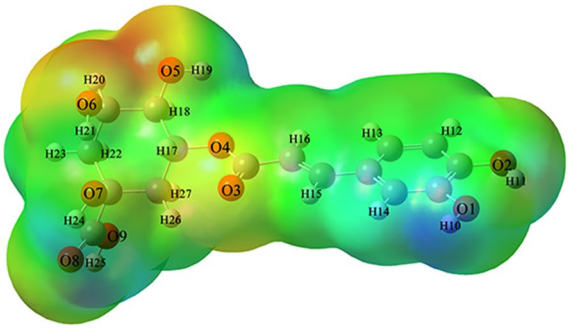

NO.	NBO	NO.	NBO	NO.	NBO
O1	-0.526	H10	0.387	H19	0.358
O2	-0.608	H11	0.382	H20	0.135
O3	-0.435	H12	0.143	H21	0.380
O4	-0.289	H13	0.116	H22	0.170
O5	-0.470	H14	0.120	H23	0.168
O6	-0.420	H15	0.148	H24	0.390
O7	-0.560	H16	0.124	H25	0.386
O8	-0.426	H17	0.192	H26	0.174
O9	-0.464	H18	0.120	H27	0.192

(a)

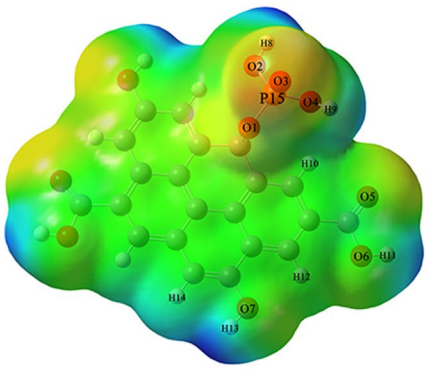

NO.	NBO	NO.	NBO
O1	-0.636	H8	0.412
O2	-0.844	H9	0.400
O3	-0.678	H10	0.170
O4	-0.820	H11	0.391
O5	-0.487	H12	0.177
O6	-0.477	H13	0.381
O7	-0.541	H14	0.115
		P15	1.972

(b)

Fig. 9 NBO charge distribution on the surface functional groups of the simulated chlorogenic acid molecule (**a**) and the modified bamboo charcoal molecule (**b**)

H11, and H13 are greater than those of H10, H12, and H14 directly connected to the carbon atoms.

Binding energy

Calculations were conducted using Gaussian 16 to analyze the interaction between the simulated chlorogenic acid molecule and the modified bamboo charcoal module. The results, which include a graphical representation and data regarding the binding energy of the molecules, are presented in Fig. 10. Notably, the interaction between the chlorogenic acid molecule and the modified bamboo charcoal module primarily involves hydrogen bonding. In structure (a), the hydrogen bond forms between the hydroxyl group of ring A on the chlorogenic acid module and the phosphate group of the modified bamboo charcoal module. In structure (b), the hydroxyl group of the ring A on the chlorogenic acid module forms hydrogen bonding with the carboxyl group of the modified bamboo charcoal module. In structure (c), hydrogen bonding occurs between the hydroxyl group on ring A of the chlorogenic acid module and the hydroxyl group of the modified bamboo charcoal module. In structure (d), hydrogen bonding occurs between the phosphate group on the modified bamboo charcoal module and the carbonyl group of rings A and B on the chlorogenic acid module. In structure (e), hydrogen bonding forms between the carboxyl group on the modified bamboo charcoal module and the carbonyl group of rings A and B on the chlorogenic acid module. In structure (f), hydrogen bonding occurs between the hydroxyl group on the modified bamboo charcoal module and the carbonyl group of rings A and B on the chlorogenic acid module. It is commonly accepted that hydrogen bonds with bond energies less than 25 kJ/mol are considered weak hydrogen bonds, those with bond energies between 25 and 40 kJ/mol are considered moderate hydrogen bonds, and those with bond energies greater than 40 kJ/mol are considered strong hydrogen bonds. In the context of the presented structures, structure (c) forms weak hydrogen bonds; structure (b) forms moderate hydrogen bonds; and structures (a), (d), (e), and (f) form strong hydrogen bonds.

Conclusion

This study conducted orthogonal experiments using a phosphoric acid solution and bamboo charcoal powder to prepare modified bamboo charcoal. The experiments involved varying the mass fraction of phosphoric acid, the impregnation ratio of bamboo charcoal powder to phosphoric acid, the activation temperature, and the activation time. The results demonstrated that modified bamboo charcoal had the strongest adsorption capacity for chlorogenic acid when impregnating bamboo charcoal in a 45% mass fraction of phosphoric acid solution, using a 1:10 ratio of bamboo charcoal powder to phosphoric acid, and activating it at a temperature of 500 °C

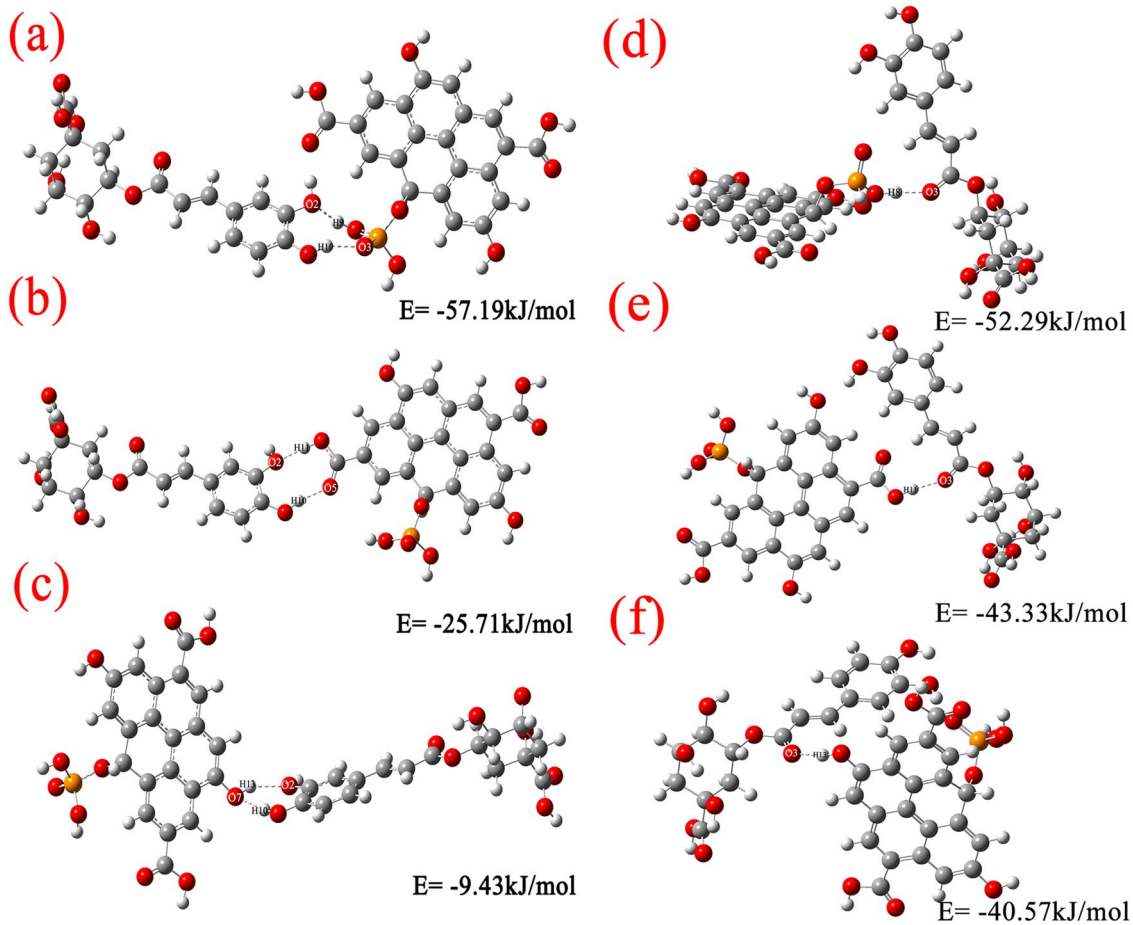

Fig. 10 Binding effect between the simulated chlorogenic acid module and the modified bamboo charcoal molecule

for a duration of 1.5 h. Under these conditions, the adsorption capacity of the modified bamboo charcoal for chlorogenic acid reached 46.8 μg, which was 46.8 times that of ordinary bamboo charcoal. Adsorption kinetic studies revealed that the curve of the modified bamboo charcoal for chlorogenic acid adhered to a first-order kinetic equation. Additionally, adsorption thermodynamic studies suggested that the curve of the modified bamboo charcoal for chlorogenic acid conformed to the Boltzmann equation.

The specific surface area of bamboo charcoal was initially 4.91 m^2/g before modification. However, after modification, it underwent a substantial increase to 115.18 m^2/g. Notwithstanding the increase, the average aperture diminished from 7.15 nm to 1.99 nm. Indeed, the heightened specific surface area primarily resulted from the presence of more micropores in the modified bamboo charcoal. The modified bamboo charcoal surface, enriched with functional groups such as phosphate, hydroxyl, and carboxyl, provided favorable conditions for enhancing its adsorption capacity for chlorogenic acid.

Through the calculations in molecular simulations, it was discovered that the addition of functional groups on the surface of modified bamboo charcoal allowed for the formation of hydrogen bonds with chlorogenic acid molecules. The binding energy observed between these molecules peaked at −57.59 kJ/mol. These results, derived from the calculations in molecular simulations, shed light on why the modification of bamboo charcoal boosts the adsorption capacity for chlorogenic acid.

This study provides valuable insights into the deep processing of bamboo charcoal and the utilization of its natural active ingredients.

Author contributions

WZ wrote the main manuscript, SZ proposed the concept and revised the manuscript, and JD conducted the experiments. All authors reviewed the manuscript.

Funding
This work was supported by the Central South University of Forestry and Technology Undergraduate Innovation and Entrepreneurship (Grant Number 202341).

Availability of data and materials
The datasets used and/or analyzed are available from the corresponding author upon reasonable request.

Declarations

Ethics approval and consent to participate
There are no ethical/legal conflicts to declare.

Consent for publication
All authors have read and approved the content and agreed to submit the paper for publication in your journal.

Competing interests
The authors declare that they have no competing interests.

Author details
[1]College of Materials Science and Engineering, Central South University of Forest and Technology, Changsha 410004, Hunan, China.

Received: 21 October 2023 Accepted: 12 January 2024
Published online: 19 January 2024

References

1. Peng MJ, Li H, Long RQ, Shi SY, Zhou HJ, Yang SP. Magnetic porous molecularly imprinted polymers based on surface precipitation polymerization and mesoporous SiO2 layer as sacrificial support for efficient and selective extraction and determination of chlorogenic acid in Duzhong brick tea. Molecules. 2018;23(7):1554.
2. Yang LG, Yin PP, Fan H, Xue Q, Li K, Li X, et al. Response surface methodology optimization of ultrasonic-assisted extraction of *Acer truncatum* leaves for maximal phenolic yield and antioxidant activity. Molecules. 2017;22(2):232.
3. Xue NN, Liu Y, Jin J, Ji M, Chen XG. Chlorogenic acid prevents UVA-induced skin photoaging through regulating collagen metabolism and apoptosis in human dermal fibroblasts. Int J Mol Sci. 2022;23(13):6941.
4. Luo J, He WY, Li X, Ji XM, Liu JB. Anti-acne vulgaris effects of chlorogenic acid by anti-inflammatory activity and lipogenesis inhibition. Exp Dermatol. 2021;30(6):865–71.
5. Ersoy E, Ozkan EE, Boga M, Yilmaz MA, Mat A. Anti-aging potential and anti-tyrosinase activity of three *Hypericum* species with focus on phytochemical composition by LC-MS/MS. Ind Crops Prod. 2019;141: 111735.
6. He XY, Zheng SJ, Sheng Y, Miao T, Xu J, Xu WT, et al. Chlorogenic acid ameliorates obesity by preventing energy balance shift in high-fat diet induced obese mice. J Sci Food Agric. 2021;101(2):631–7.
7. Williamson G. Protection against developing type 2 diabetes by coffee consumption: assessment of the role of chlorogenic acid and metabolites on glycaemic responses. Food Funct. 2020;11(6):4826–33.
8. Yamagata K, Izawa Y, Onodera D, Tagami M. Chlorogenic acid regulates apoptosis and stem cell marker-related gene expression in A549 human lung cancer cells. Mol Cell Biochem. 2018;441(1–2):9–19.
9. Zhou HL, Chen D, Gong T, He Q, Guo CQ, Zhang P, et al. Chlorogenic acid sustained-release gel for treatment of glioma and hepatocellular carcinoma. Eur J Pharm Biopharm. 2021;166:103–10.
10. Hernandez-Padilla ES, Zarate-Guzman AI, Gonzalez-Ortega O, Padilla-Ortega E, Gomez-Duran A, Delgado-Sanchez P, et al. Elucidation of adsorption mechanisms and mass transfer controlling resistances during single and binary adsorption of caffeic and chlorogenic acids. Environ Sci Pollut Res. 2022;29(18):26297–311.
11. Lu L, Cao S, Li ZX, Huang JD, Jiang YK, Deng CY, et al. Adsorption and desorption of flavonoids on activated carbon impregnated with different metal ions. RSC Adv. 2023;13(28):19235–42.
12. Zhang S, Li XZ, Zeng ZY. Study on adsorption and sustained release of *Eucommia ulmoides* Oliv. leaf extracts on activated carbon. Curr Drug Deliv. 2018;15(2):247–53.
13. Cheng S, Zhao S, Guo H, Xing BL, Liu YZ, Zhang CX, et al. High-efficiency removal of lead/cadmium from wastewater by MgO modified biochar derived from crofton weed. Bioresour Technol. 2022;343: 126081.
14. Zhang CC, Xu YH, Chen WY, Sun LY, Xu DH, Yan Y, et al. Simple and low price of monodispersed rice-like Fe2O3 supported by modified bamboo charcoal with enhanced lithium storage. J Electroanal Chem. 2018;816:114–22.
15. Fang XY, Yang M, Li JX, Xiang M, Yang KN, Wang HB, et al. Preparation of bamboo activated carbon by microwave radiation with water vapour activation and investigation of its adsorption properties. Desalin Water Treat. 2018;135:351–61.
16. Zhang Y, Wan YS, Zheng YL, Yang YC, Huang JS, Chen H, et al. Potassium permanganate modification of hydrochar enhances sorption of Pb(II), Cu(II), and Cd(II). Bioresour Technol. 2023;386: 129482.
17. Wang X, Feng JH, Cai YW, Fang M, Kong MG, Alsaedi A, et al. Porous biochar modified with polyethyleneimine (PEI) for effective enrichment of U(VI) in aqueous solution. Sci Total Environ. 2020;708: 134575.
18. Kandhavadivu P, Parthiban M. Influence of plasma treatment on moisture management of bamboo charcoal composite fabrics for hospital application. Indian J Fibre Text Res. 2022;47(1):45–58.
19. Chen XC, Wang Y, Xia HT, Ren Q, Li Y, Xu LJ, et al. "One-can" strategy for the synthesis of hydrothermal biochar modified with phosphate groups and efficient removal of uranium(VI). J Environ Radioact. 2023;263: 107182.
20. Higai D, Huang ZB, Qian EKW. Preparation and surface characteristics of phosphoric acid-activated carbon from coconut shell in air. Environ Progr Sustain Energy. 2021;40(2): e13509.
21. Ismail IS, Rashidi NA, Yusup S. Production and characterization of bamboo-based activated carbon through single-step H_3PO_4 activation for CO_2 capture. Environ Sci Pollut Res. 2022;29(9):12434–40.
22. Zhang K, Chen BL, Mao JF, Zhu LZ, Xing BS. Water clusters contributed to molecular interactions of ionizable organic pollutants with aromatized biochar via pi-PAHB: sorption experiments and DFT calculations. Environ Pollut. 2018;240:342–52.
23. Wang ZY, Hu LY, Zhao M, Dai LY, Hrynsphan D, Tatsiana S, et al. Bamboo charcoal fused with polyurethane foam for efficiently removing organic solvents from wastewater: experimental and simulation. Biochar. 2022;4(1):28.
24. Feng YX, Jin CH, Xue Q, Liu YR, Liu NN, Li ZQ, et al. Potassium permanganate and sodium silicate co-modified bamboo charcoal for efficient treatment of ammonia nitrogen pollution in rare earth mines: performance and mechanism. Water Air Soil Pollut. 2023;234(2):109.
25. Li QL, Chen TJ, Wang YL, Bryant SH. PubChem as a public resource for drug discovery. Drug Discov Today. 2010;15(23–24):1052–7.
26. Zhang SH, Wang LW, Zhang Y, Cao F, Sun Q, Ren XH, et al. Effect of hydroxyl functional groups on SO2 adsorption by activated carbon. J Environ Chem Eng. 2022;10(6): 108727.
27. Frisch MJ, Trucks GW, Schlegel HB. Gaussian 09 Revision E.01. Wallingford: Gaussian Inc; 2016.
28. Boys SF, Bernardi F. The calculation of small molecular interactions by the differences of separate total energies. Some procedures with reduced errors. Mol Phys. 2006;19(4):553–66.
29. Lu T, Chen FW. Multiwfn: a multifunctional wavefunction analyzer. J Comput Chem. 2012;33(5):580–92.
30. Humphrey W, Dalke A, Schulten K. VMD: visual molecular dynamics. J Mol Graph. 1996;14(1):33–8.
31. Pam AA, Abdullah AH, Tan YP, Zainal Z. Optimizing the route for medium temperature-activated carbon derived from agro-based waste material. Biomass Convers Biorefinery. 2023;13(1):119–30.

Publisher's Note